PROCEEDINGS OF SCIENCE

Diffractive production from the Color-Glass-Condensate

Néstor Armesto
Departamento de Física de Partículas and IGFAE, Universidade de Santiago de Compostela, 15782 Santiago de Compostela, Galicia, Spain
E-mail: Nestor.Armesto@usc.es

Amir H. Rezaeian*
Departamento de Física, Universidad Técnica Federico Santa María, Avda. España 1680, Casilla 110-V, Valparaiso, Chile
and
Centro Científico Tecnológico de Valparaíso (CCTVal), Universidad Técnica Federico Santa María, Casilla 110-V, Valparaíso, Chile
E-mail: Amir.Rezaeian@usm.cl

The diffractive production at small-x, including diffractive photo-production of vector mesons and dijet are powerful probes of non-linear gluon-saturation dynamics. We show that the t-distribution of photo-production of different vector mesons and dijet exhibit some universal features which offer a unique opportunity to discriminate among saturation and non-saturation models. Therefore, diffractive photo-production at the LHC and future colliders provides useful information about the underlying dynamics of particle production in the saturation regime.

XXIII International Workshop on Deep-Inelastic Scattering
27 April - May 1 2015
Dallas, Texas

*Speaker.

PoS(DIS2015)085

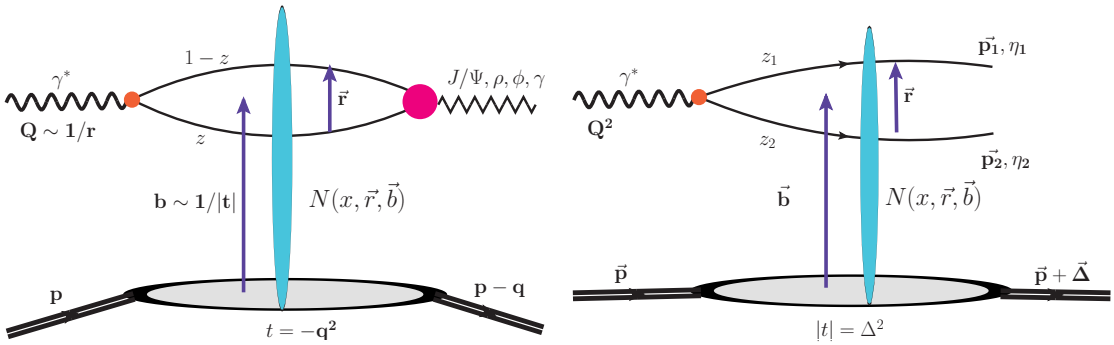

Figure 1: The color-dipole picture of diffractive production of vector mesons (left) and dijet (right).

1. Introduction

An effective field theory describing the high-energy limit of QCD is the Color Glass Condensate (CGC) [1, 2]. In the CGC approach, one systematically takes into account the non-linear gluon recombination (or saturation) and unitarity effects which are important at small Bjorken-*x*. The quest for experimental evidence of the possible signature of gluon saturation phenomenon has been the program of various past or existing experiments from HERA and RHIC to the LHC, and future experiments such as an Electron-Ion Collider (EIC) [3] and the LHeC [4]. Nevertheless, experimental evidence that can unarguably point towards gluon saturation phenomenon, has been elusive so far. This is because the experiments currently at our disposal are limited in their kinematic coverage, and often other approaches provide alternative descriptions of the same sets of data. Here, we show that diffractive production in small-x region, in particular, the measurments of t-distribution of photo-production of diffractive production provides a unique opportunity to discriminate among saturation and non-saturation models [5].

2. Exclusive diffractive processes in the colour-dipole formalism

Similar to the case of the inclusive DIS process, the scattering amplitude for the exclusive diffractive process $\gamma^* + p \to V + p$ in the CGC approach at small-x, with a final-state vector meson $V = J/\psi, \psi(2s), \phi, \rho$ (or a real photon $V = \gamma$) or a dijet $V = q\bar{q}$, can be written in terms of a convolution of the dipole amplitude $\mathscr{N}$ and the overlap of the wave functions of the photon and the exclusive final state particle, see Fig. 1. The main difference between diffractive and inclusive productions is that for the diffractive production one has to perform averaging over color sources ρ of target at amplitude level $\sigma \propto |\langle \mathscr{M} \rangle_\rho|^2$ while for the inclusive production averaging over color is performed at the cross-section level $\sigma \propto \langle |\mathscr{M}|^2 \rangle_\rho$. Therefore, in the color-dipole approach, we obtain the following generic factorization for the inclusive DIS cross-section; and for the differential cross-section of diffractive vector meson (VM) [5] and dijet [6],

$$\begin{aligned} \sigma^{DIS} &= \psi^{\gamma}_{q\bar{q}} \otimes \mathscr{N}(r) \otimes \psi^{\gamma}_{q\bar{q}}, \\ \frac{d\sigma^{VM}}{dt} &= |\psi^{\gamma}_{q\bar{q}} \otimes \mathscr{N}(r,b) \otimes \Psi^{q\bar{q}}_{V}|^2, \\ \frac{\sigma^{dijet}}{dt} &= |\psi^{\gamma}_{q\bar{q}} \otimes \mathscr{N}(r,b)|^2, \end{aligned} \tag{2.1}$$

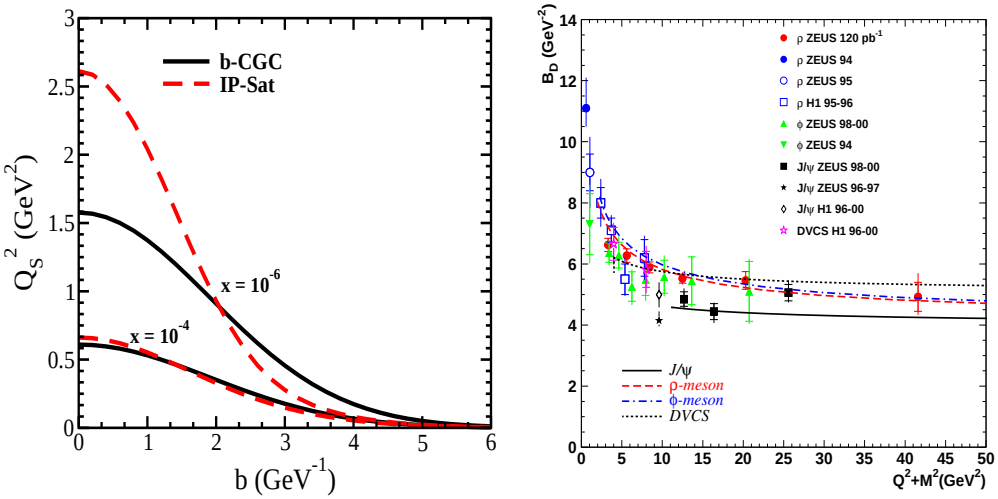

Figure 2: Left: The impact-parameter profile of saturation scale at two different Bjorken-x in the IP-Sat and the b-CGC models extracted from data shown on right panel. Right: A compilation of the value of the slope of t-distribution of exclusive vector-meson electroproduction and DVCS processes. The plots are taken from Refs. [7, 8].

with t being the squared momentum transfer $t=-\Delta^2$. In the above equation, $\mathscr{N}$ is the imaginary part of the forward $q\bar{q}$ dipole-proton scattering amplitude with transverse dipole size r and impact parameter b. Note that the impact-parameter b and t are related, namely we have $b\sim 1/|t|$. For DIS we have $t=0$, hence the integral over the impact-parameter can be trivially performed and absorbed into the over-all normalization factor. Therefore, the impact-parameter dependence of the dipole amplitude is less important for inclusive processes while it is crucial for describing exclusive diffractive ones. Note that the impact-parameter profile of the dipole amplitude entails intrinsically non-perturbative physics, and unfortunately can only be treated phenomenologically at this time. Supported by experimental data, it is generally assumed a Gaussian profile for gluons where the width of the profile, as only free parameter, is fixed via a fit to diffractive data at HERA. For the forward $q\bar{q}$ dipole-proton scattering amplitude in Eq. (2.1), we employ the impact-parameter dependent Color Glass Condensate (b-CGC) [7] and Saturation (IP-Sat) [8] dipole models which were recently updated with high precision HERA combined data, see also Refs. [6, 9]. Both models incorporate key features of small-x physics properties and match smoothly to the perturbative QCD regime at large Q^2 for a given x. In both models by construction the impact-parameter profile of the initial saturation scale is assumed to be a Gaussian, supported by the HERA data, see Fig. 2. The t-distribution at small dipole sizes can be approximately determined by the Fourier transform of the dipole impact-parameter profile. Therefore, at small dipole transverse size, in rather model independent fashion, one can directly relate the saturation scale impact-parameter profile $Q_s(x,b)$ to the t-distribution of diffractive vector mesons,

$$\frac{d\sigma_{T,L}^{\gamma^* p\to E p}}{dt}\approx e^{-B_D|t|}\ (\text{large } Q^2)\Longleftrightarrow Q_s^2(x,b)\approx Q_s^2(x)e^{-b^2/2B_D}, \tag{2.2}$$

where t-slope B_D gives the width of saturation scale distribution in proton. Note that the above expersion is only valid at large Q^2, approaching the saturation region from the dilute DGLAP regime.

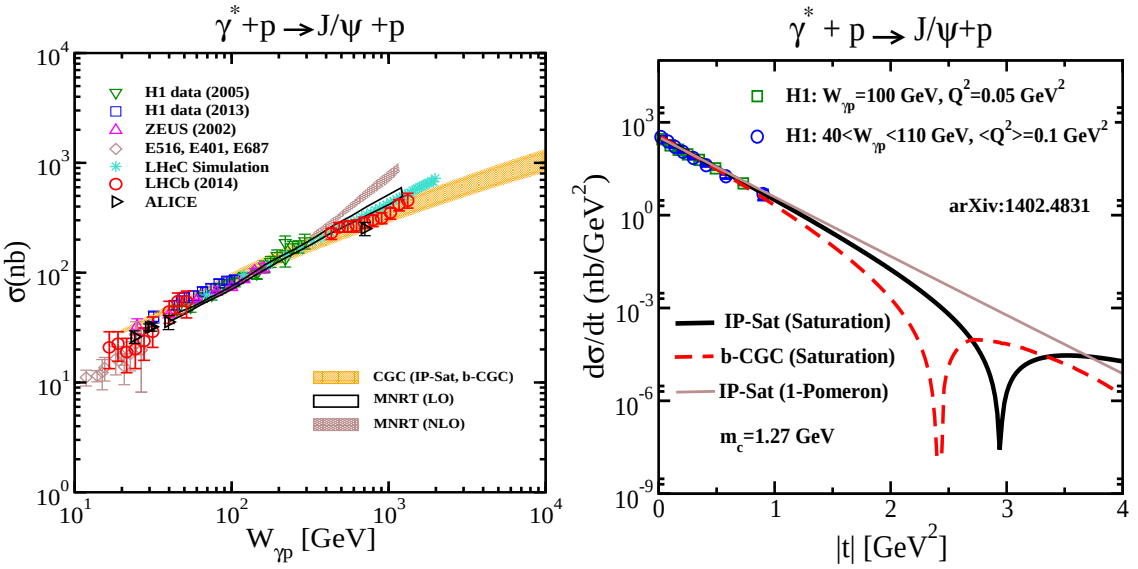

Figure 3: Left: Total J/ψ cross-section as a function of $W_{\gamma p}$, compared to results from the CGC/saturation (orange band) calculated from the b-CGC and the IP-Sat models [7, 8]. Right: Differential vector meson cross-sections for J/ψ, as a function of $|t|$ within the IP-Sat, b-CGC and 1-Pomeron models with a fixed $m_c = 1.27$ GeV at HERA. The plots are taken from Ref. [5].

At a fixed Q^2, the typical dipole size is bigger for lighter vector meson therefore the validity of the above asymptotic expression is postponed to a higher Q^2. This fact is remarkably in agreement with the recent data from HERA, see Fig. 2 right panel. The IP-Sat and the b-CGC models have been intensively applied to many reactions including heavy-ion collisions, see e.g. [10, 11]. In order to single out the implication of saturation effect, we compare our results with the 1-Pomeron model [5] which corresponds to the leading-order pQCD expansion for the dipole amplitude in the color-transparency region, as opposed to the saturation case. For the forward vector meson wave functions in Eq. (2.1), we employ the boosted Gaussian wave-function with parameters determined from normalisation, the orthogonality conditions and a fit to the experimental leptonic decay width [5]. The explicit form of forward photon and vector meson wave functions in Eq. (2.1) can be found in Ref. [5].

In Fig. 3, we compare the total J/ψ cross-section as a function of centre-of-mass energy of the photon-proton system $W_{\gamma p}$, obtained from saturation models and from a pQCD approach at leading-order (LO) and next-to-leading-order (NLO) with all available data from fixed target experiments to the recent ones from HERA, LHCb and ALICE. We also show the LHeC pseudo-data obtained from a simulation based on a power-law extrapolation of HERA data. The band labeled "CGC" includes the saturation results obtained from the IP-Sat and the b-CGC models with the parameters of models constrained by the recent combined HERA data. Note that the LHCb data points in Fig. 3 were not used for fixing the model parameters, and therefore our CGC results in Fig. 3 at high energy can be considered as predictions. The CGC band in Fig. 3 also includes the uncertainties associated with choosing the charm mass within the range $m_c = 1.2 \div 1.4$ GeV extracted from a global analysis of existing data at small-x $x < 0.01$ [7, 8]. Note that diffractive J/ψ production is sensitive to the charm quark mass at low Q^2. It is seen that the ALICE and

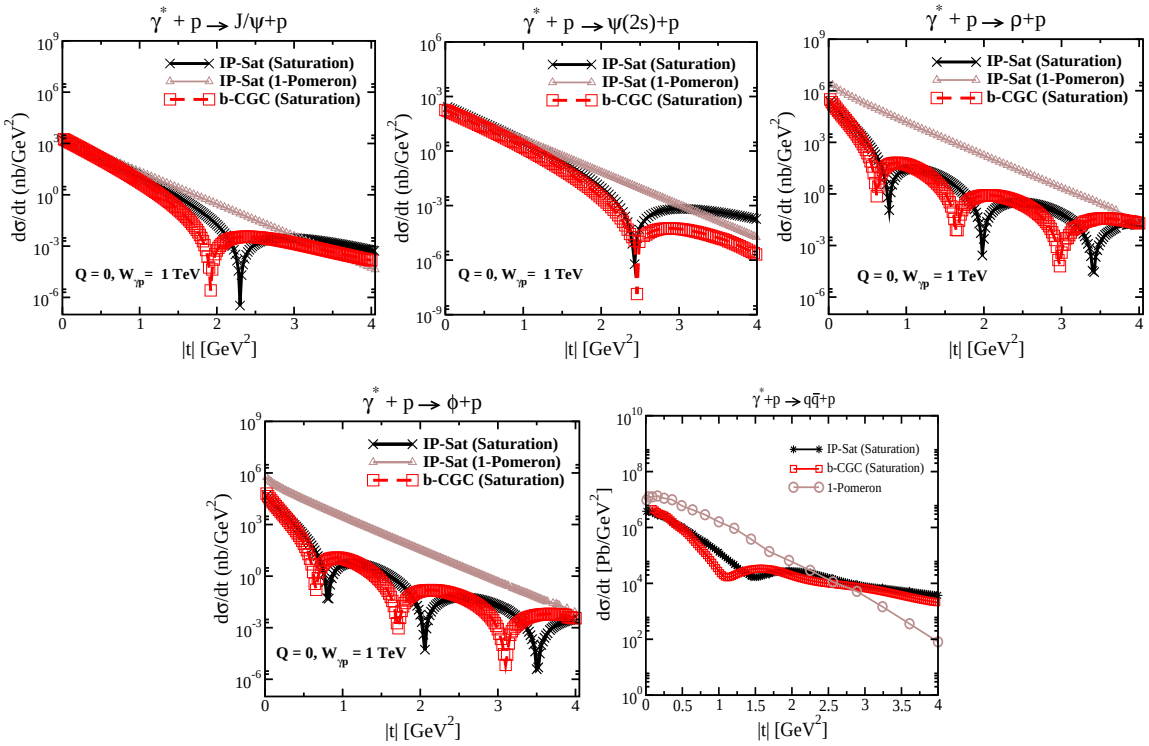

Figure 4: Differential diffractive vector meson photo-production cross-sections for $J/\psi, \psi(2s)$, ρ and ϕ, as a function of $|t|$ within the IP-Sat (saturation), the b-CGC and the 1-Pomeron models at a fixed $W_{\gamma p} = 1$ TeV and $Q = 0$. In the lower panel, we also show differential diffractive dijet photo-production cross-section at a fixed $E_p = 5$ TeV and $W_{\gamma p} = 4$ TeV for rapidities interval of two jets within $\eta_1 \in [6, 7.4]$ and $\eta_2 \in [0, 6]$. The plots are taken from Refs. [5, 6].

LHCb [12] data are in good agreement with the CGC predictions while there seems to be some tensions between the experimental data and the pQCD results (labeled MNRT LO and NLO) at high $W_{\gamma p}$ [5]. In Fig. 3, right panel, we compare the saturation and non-saturation models results for the t-distribution of the exclusive photo-production of J/ψ at $Q \approx 0$ with available data from HERA. It can be observed that at low $|t|$ where currently experimental data are available, one cannot discriminate between the saturation and non-saturation (1-Pomeron) models and all three models: IP-Sat, b-CGC and 1-Pomeron, provide a good description. However, at large $|t|$ the models give drastically different results, namely both the IP-Sat and the b-CGC saturation models produce a dip while the 1-Pomeron model does not. Note that theoretical uncertainties due to the charm mass are less important for the t-distribution than for the total cross-section.

In Fig. 4, we compare the results obtained from the IP-Sat and the b-CGC models with those from the 1-Pomeron model, for the t-distribution of the elastic photo-production (for $Q = 0$) of vector mesons J/ψ, $\psi(2s)$, ρ, ϕ and dijet $q\bar{q}$ off the proton at an energy accessible at the LHC/LHeC. Drastic different patterns for the diffractive t-distribution emerge between saturation and non-saturation models for lighter vector mesons production such as ρ and ϕ, with the appearance of multiple dips. The fact that the t-distribution of diffractive dijet production also exhibits dip-type structure within the saturation models, provide further evidence that the emergence of dip structure in the diffractive t-distribution is universal and does not depend on the details of the final-state

particle wave functions.

The emergence of a single or multiple dips in the t-distribution of diffractive vector mesons and dijet production in the saturation models is directly related to the saturation (unitarity) features of the dipole scattering amplitude $\mathscr{N}$ at large dipole sizes [5]. In the 1-Pomeron model, since the impact-parameter profile of the dipole amplitude is a Gaussian for all values of r, its Fourier transform becomes exponential for all values of t. However, in a case that the typical dipole size which contributes to the integral of cross-section is within the unitarity or black-disc limit, with $\mathscr{N} \to 1$, the Fourier transform of the dipole amplitude in impact-parameter space leads to a dip or multi-dips. The saturation effect becomes more important at smaller Bjorken-x or larger $W_{\gamma p}$, and lower virtualities Q where the the contribution of large dipole sizes becomes more important. For lighter vector mesons, the overlap extends to larger dipole sizes resulting in a dip structure. In saturation models, the dips in the t-distribution recede towards lower $|t|$ with decreasing mass of the vector meson, increasing energy or decreasing Bjorken-x, and decreasing virtuality Q. It is important to note that the main difference between a dipole model with linear and non-linear evolution (incorporating saturation effects through some specific model as those employed in this work) is that the former does not lead to the black-disc limit and, therefore, the dips do not systematically shift toward lower $|t|$ by increasing $W_{\gamma p}$, $1/x$, and r or $1/Q$, while the latter does. Non-linear evolution evolves any realistic profile in b, like a Gaussian or Woods-Saxon distribution, and makes it closer to a step-like function in the b-space by allowing an increase in the periphery of the hadron (the dilute region) while limiting the growth in the denser centre. This leads to the appearance of dips with non-linear evolution even if the dips were not present at the initial condition at low energies or for large x (e.g. a Gaussian profile), or to the receding of dips towards lower values of $|t|$ even if they were already present in the initial condition (e.g. with a Woods-Saxon type profile).

To conclude: we showed that the recent LHC data on diffractive J/ψ photo-production are in good agreement with the saturation/CGC predictions while there are some tensions between recent LHCb and ALICE data with the 1-Pomeron model and pQCD results, see Fig. 3. This can be considered as the first hint of saturation effects at work in diffractive photo-production of vector mesons off proton at the LHC. We showed that the t-differential cross-section of diffractive production of vector mesons and dijet in high-energy collisions offer a unique opportunity to probe the saturation regime and discriminate between saturation and non-saturation models, see Fig. 4. Within saturation models, the t-differential cross-section of diffractive production exhibits dip-type structure. The dip becomes stronger in a kinematic region that the saturation scale is larger, and the dip disappears in the dilute region (in non-saturation models). These features are universal and persist independent of whether the final-state is a vector meson J/ψ, $\psi(2s)$, ρ, ϕ or a $q\bar{q}$ dijet.

References

[1] L. V. Gribov, E. M. Levin and M. G. Ryskin, Phys. Rept. **100**, 1 (1983); A. H. Mueller and J-W. Qiu, Nucl. Phys. **268**, 427 (1986); A. H. Mueller, Nucl. Phys. **B558**, 285 (1999).

[2] L. D. McLerran and R. Venugopalan, Phys. Rev. **D49**, 2233 (1994); Phys. Rev. **D49**, *ibid*. **49**, 3352 (1994); *ibid*. **50**, 2225 (1994).

[3] D. Boer, M. Diehl, R. Milner, R. Venugopalan, W. Vogelsang, D. Kaplan, H. Montgomery and S. Vigdor *et al.*, arXiv:1108.1713; A. Accardi *et al.*, arXiv:1212.1701.

[4] J. L. Abelleira Fernandez *et al.* [LHeC Study Group Collaboration], J. Phys. **G39**, 075001 (2012) [arXiv:1206.2913].

[5] N. Armesto and A. H. Rezaeian, Phys. Rev. **D90**, 054003 (2014) [arXiv:1402.4831].

[6] T. Altinoluk, N. Armesto, G. Beuf and A. H. Rezaeian, under preparation.

[7] A. H. Rezaeian and I. Schmidt, Phys. Rev. **D88**, 074016 (2013) [arXiv:1307.0825].

[8] A. H. Rezaeian, M. Siddikov, M. Van de Klundert and R. Venugopalan, Phys. Rev. **D87**, 034002 (2013) [arXiv:1212.2974].

[9] N. Armesto and A. H. Rezaeian, arXiv:1407.6703; A. H. Rezaeian, arXiv:1407.5956.

[10] B. Schenke, P. Tribedy and R. Venugopalan, Phys. Rev. Lett. **108**, 252301 (2012); *ibid*., Phys. Rev. **C86**, 034908 (2012); C. Gale, S. Jeon, B. Schenke, P. Tribedy and R. Venugopalan, arXiv:1209.6330.

[11] E. Levin and A. H. Rezaeian, Phys. Rev. **D82**, 014022 (2010); Phys. Rev. **D82**, 054003 (2010); Phys. Rev. **D83**, 114001, (2011); Phys. Rev. **D84**, 034031 (2011); E. Levin and A. H. Rezaeian, arXiv:1011.3591; A. H. Rezaeian, Phys. Lett. **B718**, 1058 (2013); Phys. Lett. **B727**, 218 (2013); Phys. Rev. **D85**, 014028 (2012). A. H. Rezaeian, Nucl. Phys. **A910-911**, 450 (2013) [arXiv:1208.0026]; A. H. Rezaeian and A. Schaefer, Phys. Rev. **D81**,114032 (2010).

[12] R. Aaij *et al.* [LHCb collaboration], J. Phys. G: Nucl. Part. Phys. **41**, 055002 (2014); B. B. Abelev *et al.* [ALICE Collaboration], arXiv:1406.7819.